COBEM 2021 26th International Congress of Mechanical Engineering
ABCM Associação Brasileira de Engenharia e Ciências Mecânicas
November 22-26, 2021, Virtual Congress, Brazil

COB-2021-0599
STARTUP FLOW VISUALIZATION OF VISCOPLASTIC MATERIAL IN THE PRESENCE OF WALL SLIP

Angel De J. Rivera Jimenez
Yamid J. Garcia Blanco

Eduardo Matos Germer
Admilson T. Franco
Federal University of Technology-Paraná - UTFPR, Research Center for Rheology and Non-Newtonian Fluids - CERNN, 81280-340, Rua Deputado Heitor Alencar Furtado 5000 - Ecoville, Curitiba-PR, Brazil
angeljimenez@alunos.utfpr.edu.br, yamidblanco@alunos.utfpr.edu.br, eduardomg@utfpr.edu.br, admilson@utfpr.edu.br

Abstract. *Viscoplastic materials are characterized by the presence of a critical stress value below which there is no flow, and a decrease of the apparent viscosity occurs when shear stress imposed is above this critical stress. Despite the complexity of viscoplastic materials, they are widely used in several industrials segments, such as polymer injection molding processes, food pumping, debris flow, cementing horizontal wells, and processes in the waxy crude oil industry. During shut down situations of the crude oil transportation caused by emergency or maintenance activities, the crude oil in rest exhibits a gel-like structure after a period of time. In order to restart the flow, high pressures are applied, which can cause risks of damage to the transport pipeline network and can compromise the operation. To prevent these risks, the pipeline dimensions are overestimated reflecting high infrastructure costs that sometimes make projects unviable. Therefore, an accurate prediction of the minimum pressure to restart the flow is necessary as an operational requirement. The objective of this experimental study is to investigate and visualize the startup flow of yield stress materials in the pipeline. The velocity profiles, the presence of plug structure and the solid-fluid transition are analyzed before and during the yielding of the fluid. For a better understanding of the flow dynamics of these materials, a test section of length 0.980 m with a circular cross-section of inner radius 0.011 m was attached to two reservoirs to control the inlet and outlet pressure. A 2D-Particle Imaging Velocimetry system is used as visualization setup. An aqueous ultrasound gel solution (25 wt%) is used as viscoplastic material. A previous validation stage was carried out using a glycerine solution as a Newtonian fluid. The validation test was performed in the laminar regime. The velocity profiles were compared with the analytical solutions for Newtonian fluid in a transient laminar flow regime. To verify the startup flow, constant pressure values were applied for a period of 600 seconds, and pressure measurements were obtained by pressure transducers located at the inlet and outlet of the test section. A relationship between the minimum startup flow pressure drop and velocity field evolution is observed. Also, the time required to restart the line blocked depends mainly on the applied pressure drop and the viscosity that decreases with time. Finally, it was observed that a slip velocity is presented during the restartup flow, which can be scaled as a power-law relation with the shear stress at the wall and the wall velocity gradient.*

Keywords: *Viscoplastic materials, wall slip, star-up flow, PIV*

1. INTRODUCTION

The viscoplastic fluids are used in several major industries, and from a practical perspective, such materials have found an increasing number of applications, which include foods, cosmetics, oil field, etc (Alba and Frigaard, 2016; Burfoot *et al.*, 2009). Also, they are encountered in daily life in various forms such as hair gels, emulsions, food pastes, and mud (Fryer *et al.*, 2006; Cole *et al.*, 2010). The understanding of viscoplastic fluid flows is essential in some industrial processes like the flow of waxy crude oils, debris flows, and flows in the food industry (Phillips *et al.*, 2011; Coussot and Meunier, 1996; Curran *et al.*, 2002).

After flow interruptions in these industrial processes, whether for operational or emergency reasons, the fluid at rest in the pipeline shows gel-like behavior (El-Gendy *et al.*, 2012). Such is the case of waxy crude oil that, when exposed to a cold environment during transport through long pipelines, loses heat and a gel-like structure is formed due to its waxy composition (Sierra *et al.*, 2016). Under such conditions, startup flow could be unsafe, as the pumping system needs to provide the pressure necessary to break the gel structure and resume the flow, called the startup pressure. Normally, the restart pressure is higher than the operational one due to the viscoplasticity of the fluid.

The viscoplastic fluids behave as a solid when the shear stress is below the yield stress (τ_y) (Dalla *et al.*, 2019), but they

flow when the shear stress exceeds the τ_y value. Considering that the minimum pressure for the startup flow is correlated with the yield stress of material (Coussot, 2014), a large number of studies devoted to the yielding of viscoplastic fluids in rheometric flows have been performed (Roberts and Barnes, 2001; Putz and Burghelea, 2009; Møller *et al.*, 2009; Benmouffok-Benbelkacem *et al.*, 2010), contrary to the few numbers of experimental studies focused on the startup visualization. Experimental studies performed by Poumaere *et al.* (2014), Sierra *et al.* (2016), and Huilgol *et al.* (2019) revealed the existence of three flow regimes. Initially, an elastic behavior similar to that found in solids was observed, being characterized by the dependence of stress and shear deformation. Immediately a solid-liquid state coexistence phase is observed, and finally, a completely viscous regime is reached, which is maintained in the remaining flow.

In this work, the startup flow is studied in a straight pipe configuration. Constant pressure values were imposed on the ultrasound gel solution (25 wt%) and subsequently displacing it and causing it to yield. We measured the pressure in the viscoplastic material and using the particle image velocimetry (PIV), the transient flow field of the fluid was studied. For the flow conditions and geometries used, the results are consistent with the yielding process described by Putz and Burghelea (2009), it was observed that the transition between the solid-like regime and the fully yielding regime is not direct, but mediated by the coexistence of a solid-liquid regime. The presence of wall slip is observed and reveals that it is a phenomenon present in the startup viscoplastic flow, which increases with the shear stress on the wall.

2. EXPERIMENTAL SETUP AND METHODOLOGY

2.1 Fluid preparation

Ultrasound gel composed of Carboxyvinyl Polymer (Carbopol®) was used as yield stress fluids. Due to their low thixotropy, excellent micro-structural stability, optical transparency, highly reproducibility and stable rheological properties, Carbopol gels has been considered as model yield stress fluid (Buscall, 2010).

For fluid preparation, initially, 8.5 kg of deionized water was weighed on a precision balance. Subsequently, 3 kg of ultrasound gel was added, representing 25% of the total weight of the mixture, then 6 g of sodium benzoate was also added to balance the pH and prevent the proliferation of bacteria, which could affect the properties of fluid. The mixture was stirred for 6 hours, to ensure homogeneity. The final pH and density values were set in 7.31 and 1014 kg/m3, respectively. For identification issues, the ultrasound gel 25 wt% solution was named fluid C-25.

2.2 Rheological testes

To analyze the rheological behavior of the viscoplastic fluid used in this study, rheometric tests of steady flow curve and creep flow were performed. The procedure to perform each test is described below, and the results obtained are presented in the section 4.

To perform the flow curve tests, a HR-3 rotational rheometer (TA Instruments) was used. The rheological tests were carried out at a temperature of 22 ºC, in order to represent the same conditions in the laboratory. A smooth parallel plate (S-PP) geometry was used to perform the tests, and decreasing shear rate ramps were applied from 100 to 0.02 s^{-1}. The data obtained with the rheometer were adjusted using the Hershel-Bulkley model, given by:

$$\tau = \tau_y + k\left(\dot{\gamma}\right)^n \tag{1}$$

where τ_y is the yield stress, n is the shear thinning index, and k is the consistency index.

In order to determine the behavior of the fluid before the starting flow, creep tests were carried out, which consisted of applying constant homogeneous shear stress and then measuring the variation of the resulting shear rate with time. The rheological tests were performed at a temperature of 22 ºC and using a rotational HR-3 rheometer (TA Instruments). Two geometries were used to evaluate the effects of slip on the applied shear stress: S-PP and cross-hatched parallel plates (CH-PP). The measurements were carried out according to the following protocol: initially, the fluids were left at rest for a time of 120 seconds (s), at the end of rest time, shear stress is applied to the material for the time of 600 s, determined as enough time to verify the material flow. After the imposition time, the fluid was again left at rest for another 120 s. The same procedure was repeated for various values of shear stress.

2.3 Experimental Setup

An experimental setup was designed to study the startup flow of fluid C-25. Figure 1 shows a schematic illustration that identifies the main components and the subcomponents of the experimental setup. The device is basically made up of two systems: hydraulic and control/acquisition. The hydraulic system is integrated into three parts: the main pipe (C), two auxiliary sections (B), and two reservoir tanks (A). These tanks were identified a the external tank and the internal tank. Therefore, the tank placed before the test section (right) was named the external reservoir tank (or external reservoir), and the opposite side (left) internal reservoir tank (or internal reservoir). Both tanks had a quick coupler adapter on the top cap for filling with compressed air, and also had a manometer (K), a pressure relief valve (J). Finally, to visualize the level

variation in the tank due to the startup flow a level sight glass was installed (H). To record the pressure difference during the flow restart, two pressure sensors (D) were used. Temperature monitoring is done by four thermocouples (F).

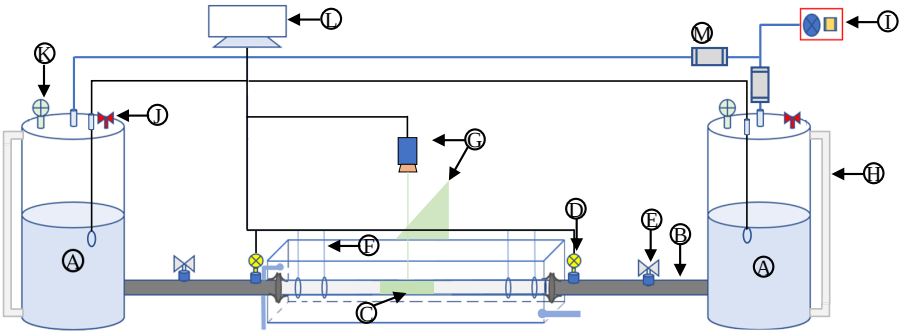

Figure 1. Schematic illustration of the components of the experimental setup.

The pressurization system consisting of a pressure regulator and a manometer (I), and two solenoid valves (M) were connected to the compressed air system of the CERNN's LabFlow, allowing to impose the pressure required for startup flow during the tests. The pressure values imposed were controlled through a program developed in LabVIEW, which allowed the set pressure values to be applied with greater precision.

The visualization of viscoplastic fluid flow through the experimental setup is possible using a particle imaging velocimetry (PIV) technique. In this study, spherical glass tracer particles with a diameter of 10 μm were used to visualize the flow. The particles absorb light at a wavelength of 532 nm and emit it back at 532 nm. Figure 2 shows the setup for using the PIV, a laser system of 60 mJ is synchronized with a CMOS camera by a synchronization box. A visualization plane is obtained after setting the camera at 90 degrees with the laser beam.

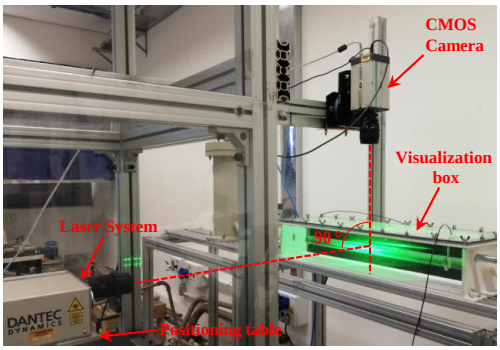

Figure 2. Visualization system setup. The plane of the laser beam and the visualization plane of the camera is set in a perpendicular configuration.

In order to record the exact moment of the flow restart, the visualization system is activated 10 seconds before the regulator valve is opened. The inlet pressure, the pressure drop, mean velocity, and temperature data are recorded and synchronized with the image acquisition system. The pressure data are recorded until 600 s after the image recording is stopped.

3. METHODOLOGY VALIDATION

The PIV methodology in transient regime flows was validated with a test performed with glycerine as Newtonian fluid. The velocity profiles were obtained for a pressure drop along the test section and compared with the analytical solution for velocity and for Newtonian fluid (WATSON, 1995) given by the Fourier-Bessel solution and expressed as:

$$u(r,t) = \frac{R^2 \Delta p}{4\mu L}\left[1 - \left(\frac{r}{R}\right)^2\right] - \sum_{n=0}^{\infty} C_n J_0(\lambda_n r) e^{-\lambda_n \frac{\nu t}{R^2}} \tag{2}$$

where Δp is the pressure drop between two points along the test section with a distance L, R is the radius of the pipe, μ is the dynamic viscosity, ν the kinematic viscosity, r radius, J_0 and J_1 are the zero and first Bessel function, respectively.

The (λ_n) variable represents the eigenvalues calculated for the respectively Bessel functions, and t is the variable of time. The coefficients C_n are expressed as:

$$C_n = \frac{8R^2}{\lambda_n^3 J_1(\lambda_n)} \tag{3}$$

Figure 3 compare the velocity profiles obtained by the flow visualization with the analytical profiles obtained by Eq. (2) at different times for a Re =1 and pressure drop of 911 Pa.

The validation stage shows that despite the refinement limitations of PIV technique at the wall region, the methodology used has a good agreement with the analytical solution for Newtonian fluid flows in straight pipes for different instants of time.

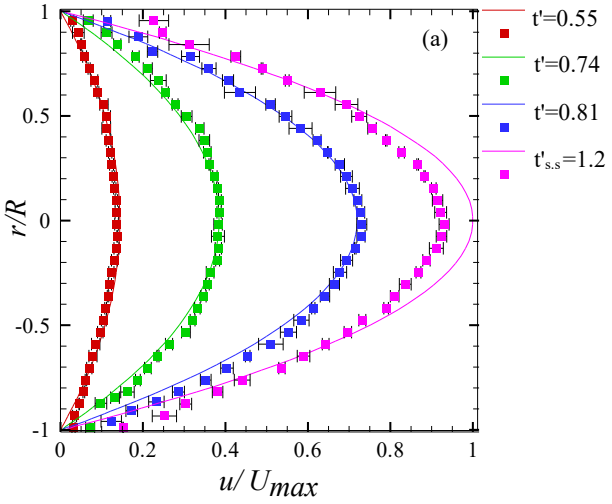

Figure 3. Comparison between the evolution of the dimensionless velocity profiles u/U$_{max}$ experimental (solid symbols) and analytical solution Eq. (2) (solid line) for a Δp 911 Pa (R$_e$ = 1) and different dimensionless times.The error bars are defined by the root mean square deviation of the velocity profiles and the error of the PIV technique. Figure t$_{s.s}$ represents the steady-state.

The dimensionless time ($t\,'$) used for the validation and the experimental tests consisted of dividing the dimensional time scale (t) by the value of time until reaching the set wall shear stress, which was denominated critical time (t_c), in this way a dimensionless time scale $t\,'$ from zero to one (0-1) was obtained, which allow compararing the transient process of the fluids. This dimensionless time scale is described by Eq. (4)

$$t' = \frac{t_c}{t} \tag{4}$$

4. RESULTS

This section presents the rheological results of fluid C-25. The constant flow curves obtained from the experimental setup are compared with the rheometric data. Finally, the flow kinematics using the PIV technique, the analysis of the sliding behavior of the wall as a function of the wall shear stress and the calculation of the wall shear stress through the velocity profiles are exposed and discussed.

4.1 Rheological measurements

The analysis begins with the steady flow curves of the materials. The results obtained in the experimental setup were compared with the data from the HR-3 rotational rheometer (TA Instruments). To obtain the steady flow curve show in Fig. 4 a, seven shear rates were used. It is observed that the curves have similar trends, however, the difference of the shear stresses in the range of measured shear rates is practically constant and the absolute percentage error between the adjustments was 60.6%, which is considered high. A possible explanation for these discrepancies between the results obtained in the experimental setup and the rheometric tests is the existence of wall slip. Then, based on the evidence that there is wall slip in the results obtained from the experimental setup and looking to obtain a better correlation with the data from rheometric measurements, the correction presented by Weissenberg-Rabinowitsch (WRC) (Macosko, 1994), Eq. (5), and new shear rate values were obtained and a new steady flow curve was plotted (Fig. 4 b).

$$\dot{\gamma}_{corr} = \frac{\dot{\gamma}_{aw}}{4}\left(3 + \frac{\mathrm{d}\ln Q}{\mathrm{d}\ln \tau_w}\right) \tag{5}$$

where $\dot{\gamma}_{aw}$ and τ_w are the apparent shear rate and the shear stress in the pipe wall, respectively, Q is the volumetric flow rate measured in m^3/s. The term $d\ln Q/d\ln\tau_w$ is the inclination of $\ln Q$ as a function of $\ln\tau_w$, for each point. For Newtonian fluid, the inclination is 1. For non-Newtonian fluids, the function can be expressed by $\ln Q = a\ (\ln\tau_w)^2 + b\ \ln\tau_w + c$, where a , b and c are constants that can be adjusted for each case.

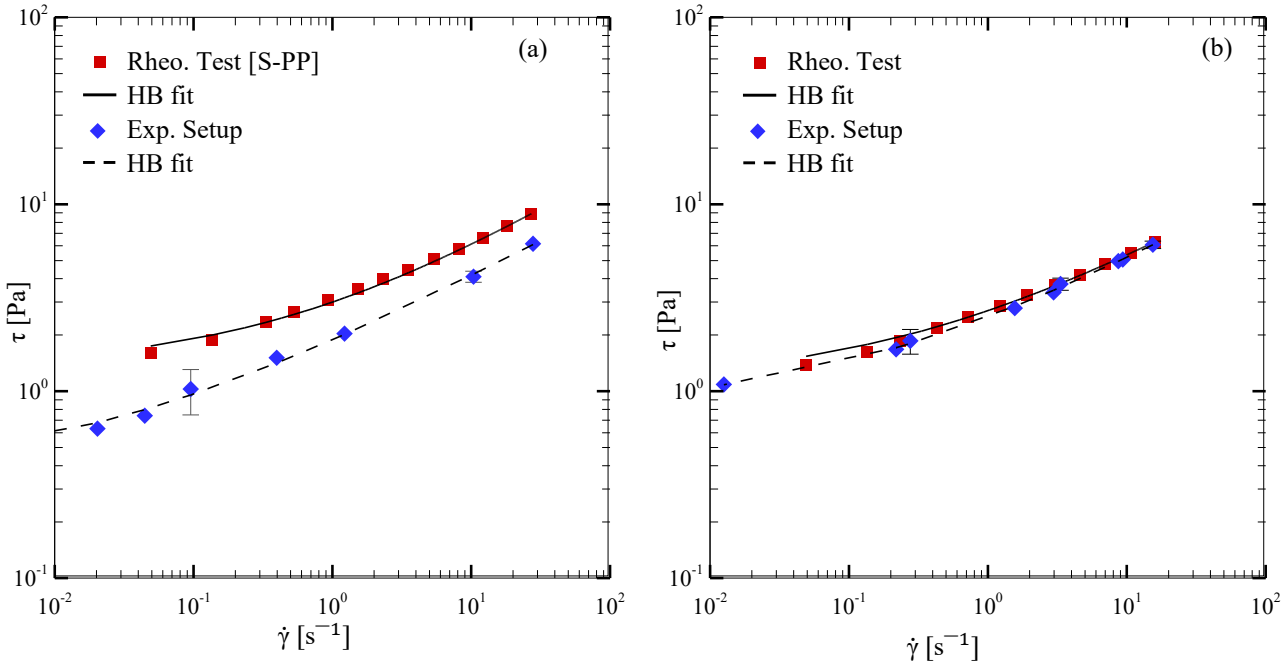

Figure 4. Steady flow curves for the fluid C-25 using S-PP geometry obtained by rheometric measurements and tests in the experimental setup (a) without slip correction and (b) with WRC slip correction. The error bars are defined by the uncertainty of the calculation of the wall shear stress.

From constant flow curve results, it was obtained that the yield stress is equal to 1.22 Pa.

A yield stress of 1,22 Pa was obtained from the flow curve results. In order to determine the behavior of the fluid before startup flow creep tests were performed. Figure 5 presents the results of the creep flow tests for the two fluids used. It can be observed that the value of shear stress for which the shear rate tends to a non-zero value varies with the geometry used. The results for the fluid C-25 with S-PP (Fig. 4 a) show that when the shear stress is equal to 2 Pa, the shear rate tends to a constant value, although for the stress equal to 1 Pa, the shear rate does not tend monotonically to zero and can also be considered as a startup flow shear stress value, which coincides with the results obtained for CH-PP (Fig. 5 b). Based on the results of Fig.5, the yield stress value τ_0 = 1 Pa for the fluid C-25 was adopted.

From Fig.5, three different deformation regimes were identified, consistent with previous investigations ((Benmouffok-Benbelkacem *et al.*, 2010) (Poumaere *et al.*, 2014)). These regimes were determined considering the final behavior of the fluid for each value of applied shear stress between 0 seconds and 600 seconds. The dashed lines in Fig.5 delimit the analyzed time period. For shear stress values lower than the yield stress, the variation of the shear rate tends to zero; this corresponds to a solid behavior of the material (region (S) in Fig.5). When the shear stresses more significant than the yield stress, determined as τ_0= 1, the shear rate increases monotonically for a constant value, indicating that the material fully yielded (region (F) in Fig.5).

It is observed that for values of shear stress that slightly exceed the yield stress, the shear rate reaches a peak and then decreases, remaining at a moderately constant value. This behavior is shown for the fluid and is consequent with the coexistence of regimes (region (S + F) in Fig.5), in which the fluid does not behave as a solid-like, nor as a fluid, indicating that the startup flow is not direct, but it is a transition process between the solid and fluid phases.

4.2 Temporal evolution of the velocity fields

The focus is on the temporal evolution of the velocity for a better understanding of the viscoplastic fluid's yield transition. The results were obtained by applying eight values of wall shear stress. However, for practicality, the temporal analysis is shown for three values of τ_w, chosen as critical for two reasons: 1) they are values close to the yield stress calculated by creep tests, and 2) fluid displacement was visualized during the increase of wall shear stress to a set value.

Figure 6 shows velocity field behavior for fluid C-25. Figure 6a to 6f show the evolution of the velocity field for τ_w= 0.43 Pa. It is observed that the dimensionless velocity $u/\bar{U}$ values fluctuate between a dimensionless time and another,

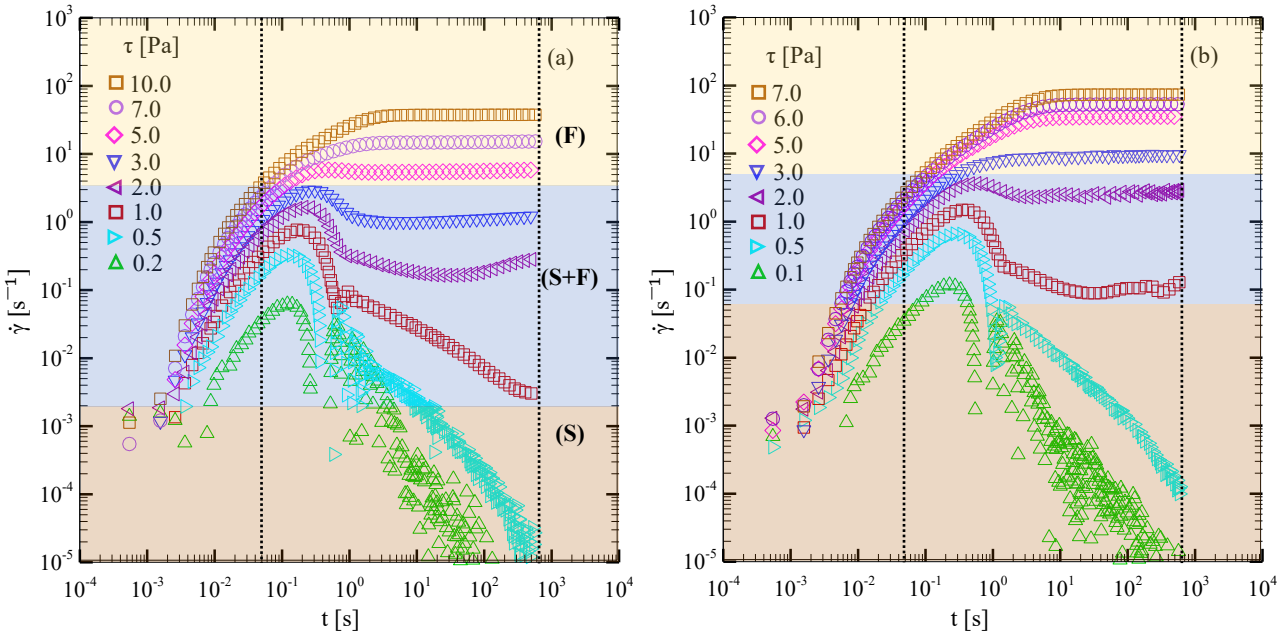

Figure 5. Creep flow tests using two types of geometries and applying different values of shear stress for the fluid C-25 a) S-PP, b) CH-PP. The symbols marking the highlighted regions denote the deformation regimes and are explained in the text: (S), solid; (S + F), solid-fluid coexistence; (F), fluid.

this is more notable for Fig. 6b and Fig. 6d, where the dimensionless velocity reaches values of 1.2×10^{-3} and 2×10^{-3} (color bar) respectively, but immediately this value decreases as shown in Fig. 6c and Fig. 6e. This behavior is similar for the velocity fields shown in Fig. 6g to 6l, measured when a τ_w= 1.02 Pa is applied. The $u/\bar{U}$ values shift between 0 and 1.5×10^{-3}, which is moderately less than τ_w= 0.43 Pa.

Figures 6m to 6r, present the results obtained for τ_w= 1.5 Pa, apparently the behavior of the velocity field shown with the two previous values of τ_w, it is only noticeable in the early dimensionless times. This leads to the conclusion that the fluctuations are originated from low or close to the yield stress τ_0 values. However, for wall shear stresses greater than τ_0, this behavior is less evident or practically disappears. Due to the limitations of the PIV technique for transient phenomena, it is not possible to quantify the value of the fluctuation of the velocity field for each dimensionless time. However, these breakthroughs are consistent with the reported by Putz and Burghelea (2009), Poumaere *et al.* (2014) and Liu and de Bruyn (2018), when performing tests in experimental and rheometric settings, respectively.

A necessary data that was visualized in the velocity fields for the two fluids, that was the presence of static zones or with very low velocity (box of dashed line) for the ratio $r/R = \pm0.5$. The following statement cannot be assured, because it is beyond the scope of the resolution of the PIV technique used, but could be slip zones on the wall and according to Bingham (1922) could be the slip layer and "slip comes from a lack of adhesion between the material and the shearing surface. The result is that there is a layer of liquid between the shearing surface and the main body of the suspension". Taghavi *et al.* (2012), also observed these areas in the study of viscoplastic fluid displacements using the UDV technique, although in greater dimension and accuracy. Some problems caused by slip were discussed in the rheological results, but it was not possible to verify these sliding areas; the results obtained by the PIV technique allow "visualize" the existence of areas over which the fluid can slide. The graphs of the velocity profiles presented in the next section will allow us to understand a broader vision of what is observed in the velocity fields.

4.3 Temporal evolution of the flow regimes in the presence of wall slip

To better appreciate the variations in the velocity fields, this section presents the evolution of the velocity profiles for several wall shear stresses. For the sake of simplicity, the results are presented only for three dimensionless times, t'=0.74, t'=0.94, and t'=15. The first is related to the wall shear stresses below the yield stress [region (S) in Fig. 5]. Figure 7a and Fig. 7d show that the velocity profiles for the fluid C-25 at t'=0.74 and t'=0.94 are irregular and fluctuate for $u/\bar{U}$=0 and $u/\bar{U}$= 2.5×10^{-3}, reaching negative values in some cases, as observed for the velocity profile (blue symbols). This negative value is related to reversal flow and possibly caused by the elastic-recoil effect of the material. Similar behavior was reported by Poumaere *et al.* (2014), in the investigation of unstable pipe flows for Carbopol® gels, and also previously reported by Benmouffok-Benbelkacem *et al.* (2010) in rheometric studies, indicating that the elastic effects of material play an essential role in the yield transition of viscoplastic fluids.

The second flow pattern is observed when the applied wall shear stresses exceed the yield stress. The velocity profiles

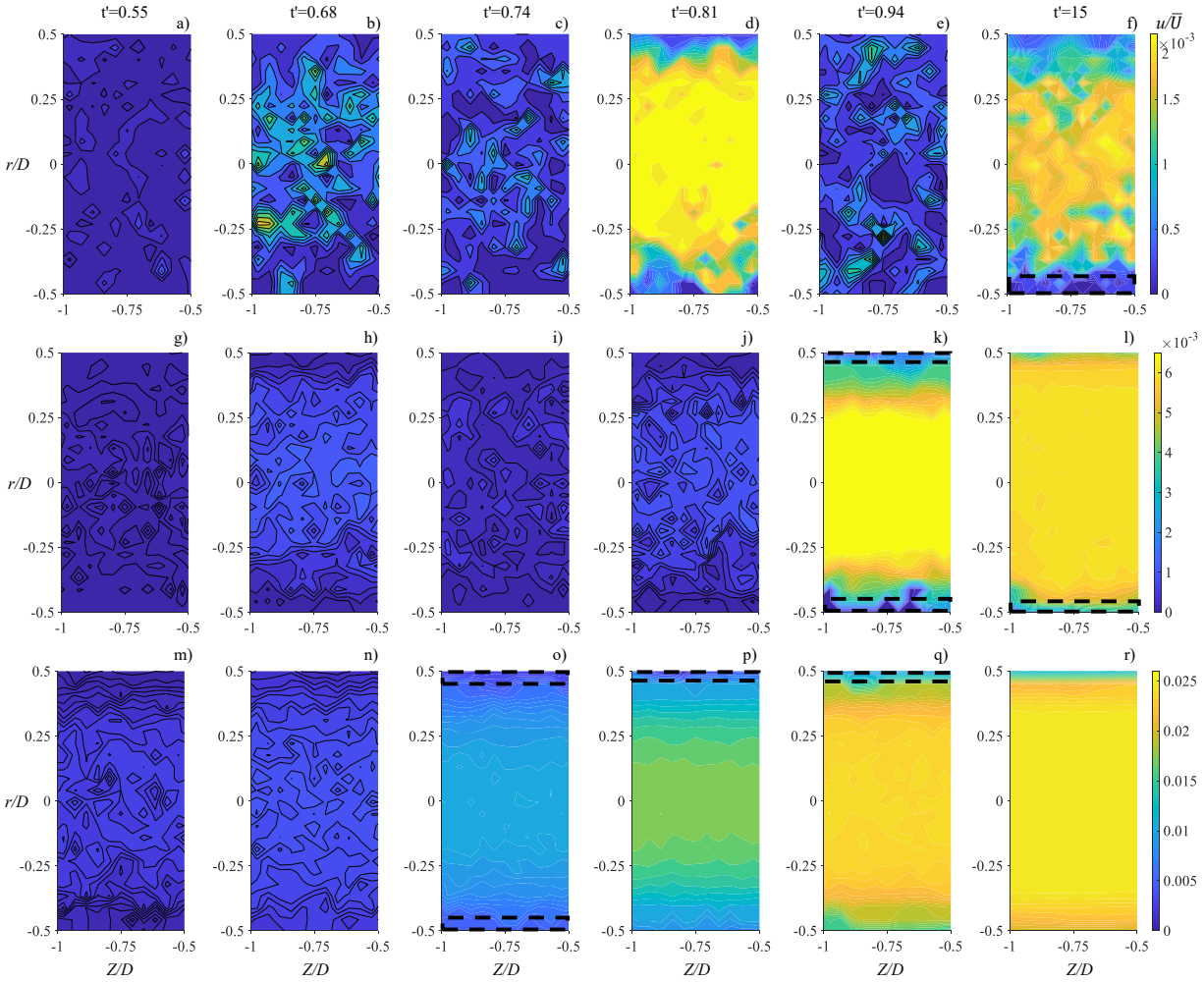

Figure 6. Velocity fields for the fluid C-25, measured as a function of time for: a)-f) τ_w=0.43 Pa; g)-l) τ_w=1.02 Pa, and m)-r) for τ_w=1.5 Pa. The values of velocity and time are dimensionless.

of Fig. 7b, Fig. 7e, and Fig. 7h show a flat or plug-like zone around the centerline of the pipe and a partially yielded region near the pipe wall, due to large values of the velocity gradients.

Finally, the fluid C-25 (Fig. 7i) yielded completely, and the radius of central plug-like decreases, qualitatively indicating that the flow corresponds to the fluid regime (F) observed in the tests of Fig. 5. As a quantitative argument, it is observed that in the framework of a yield stress fluid, the velocity profiles of Fig. 7i are fitted with good agreement with the Hagen–Poiseuille flow of a Herschel–Bulkley fluid described in Damianou *et al.* (2014), with absolute percentage error (APE) of 4%.

Concerning the wall slip of viscoplastic flows in acrylic pipe analyzed in the present study, it is observed that the dimensionless slip velocity u'_s continues to increase beyond the yield stress and as a function of the wall shear stress, as reported by Pérez-González *et al.* (2012). For the values of u'_s obtained, it is observed that the fluid C-25, when τ_w=2.03 Pa is applied at t'=0.94, has a the dimensionless slip velocity u'_s=0.058 and for τ_w=6.15 Pa at t'=15, u'_s=0.65, which is an order of magnitude greater, and represents 77.3% and 32.5% of the total dimensionless velocity, respectively.

4.4 Slip velocity behavior

Wall slip is quantified by the relative fluid-solid velocity at the interface. Section 4.3 presented the estimation of the slip velocity for the several flow conditions analyzed and a dependency relationship between slip velocity and wall shear stress was observed. In this section, the dependence of the wall slip velocity is scaled with the wall shear stress. The scale laws obtained are compared with the results of other works.

In Figure 8 it is initially observed that for t'=0.74 in the region (S), the slip velocity does not show a relationship between the data. For t' = 0.94, the slip velocity in the region (S) is slightly constant, possibly because the fluid is not affected by the stress value applied in the first instants. Beyond the region (S) at t'=0.94, the slip velocity data correlates

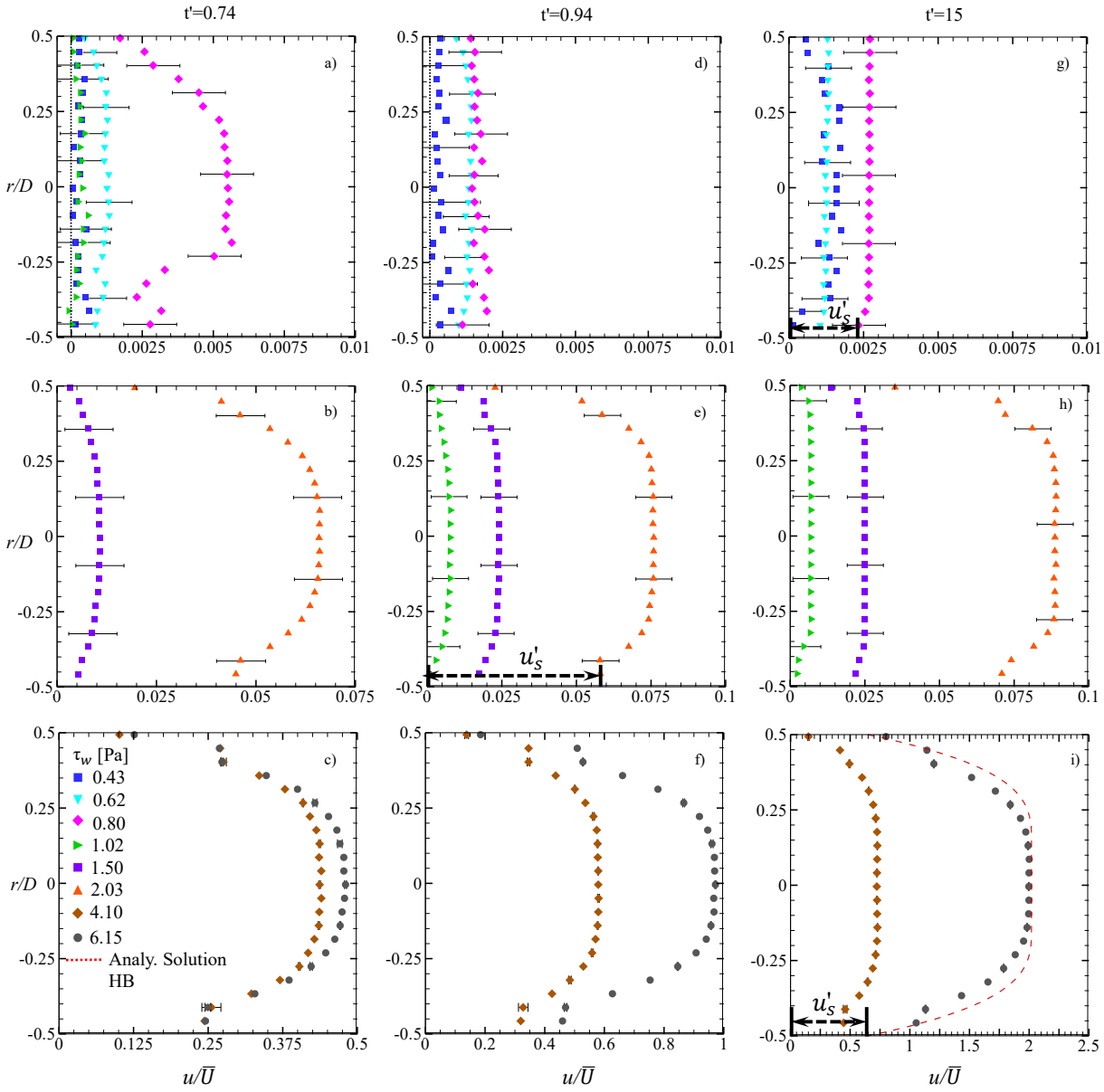

Figure 7. Evolution of velocity profile ($u/\bar{U}$) for the fluid C-25 measured in three dimensionless times: a), b), c) for t'= 0.74; d), e), f) for t'= 0.94, and g), h), i) for t'= 15. u'_s is the slip velocity dimensionless by the mean velocity ($u_s/\bar{U}$). The error bars are defined by the root mean square deviation of the velocity profiles and the error of the PIV technique.

with good agreement, that is, in the regions (S+F) and (F) and is scaled as $u_s \propto {\tau_w}^{1.52\pm0.22}$. Finally, for t' = 15, a similar behavior is observed for the solid-like regions and the slip velocity between the transition and fluid zones is scaled as $u_s \propto {\tau_w}^{1.13\pm0.04}$, it is observed that the fits overlap and indicate the beginning of the region (F), where the fluid is entirely viscous. These results are in good agreement with the results reported by Poumaere *et al.* (2014), $u_s \propto {\tau_w}^{1.32\pm0.26}$. It is generally observed that the power-law scales are almost linear, which is in good agreement with the assumption that the binder fluid is Newtonian.

According to these results, it is possible to affirm that there is a relationship between the slip velocity and the wall shear stress, and under the assumption that this relationship exists due to a depleted layer of width (δ) that prevents the fluid from adhering to the solid limit (Bingham, 1922), the correlation proposed by Kalyon (2005) (Eq.(6)) is used to obtain a simple phenomenological scale of the behavior of the sliding of the wall of the viscoplastic fluid.

$$u_s = \beta(\tau_w)^{\frac{1}{n_b}} \tag{6}$$

where β relates the width of the slip layer δ to the consistency index k_b, and the power-law index n_b of binder fluid. As Carbopol® is considered as a jammed system of swollen gel microparticles (Piau, 2007), and the solvent used to obtain the fluids was distilled water ("binder fluid"), it is considered Newtonian fluid, then k_b=1$\times10^{-3}$ Pa.s and n_b=1.

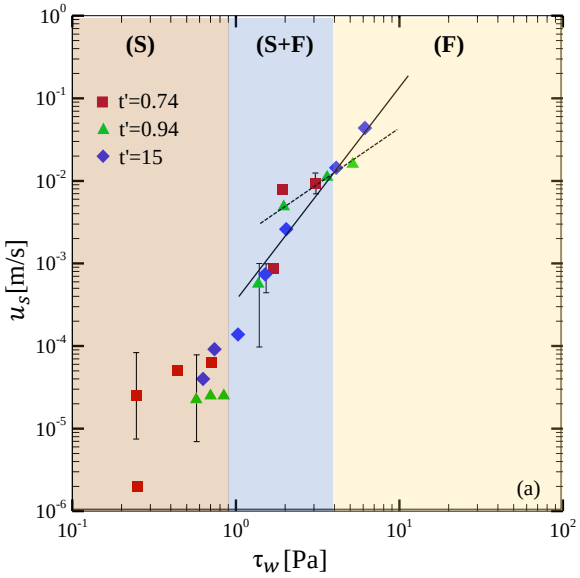

Figure 8. Dependence of the wall slip velocity on the wall shear stress at three dimensionless times for fluid C-25. The full and dashed line in Figure represents the power-law fit at t'= 15, $u_s \propto {\tau_w}^{1.13\pm0.04}$ and t'= 0.94, $u_s \propto {\tau_w}^{1.52\pm0.22}$, respectively. The error bars are defined by the root mean square deviation of the slip velocity and the error of the PIV technique.The symbols marking the highlighted regions denote the deformation regimes and are explained in the text: (S)–solid, (S+F)–solid–fluid coexistence, (F) – fluid.

In this study the factor β measured for the fluid C-25 is β=1.01$\times10^{-4}$ mPa.s^{-1}, which leads to a slip layer thickness $\delta\approx$0.101μm. The thickness of the slip layer found is of the same width order as reported by Poumaere *et al.* (2014), ($\delta\approx$0.23μm). The estimation of the thickness of the slip layer was carried out for t'=15. However, the thickness of the slip layer calculated by simple estimates is too small to be directly visualized from the flow images, and the hypothesis underlying the prediction of this scale is simply hypotheses for now.

5. CONCLUSIONS

In the present work, the startup flow of a viscoplastic material in a smooth pipe with the presence of wall slip were analyzed using different flow conditions given by the imposition of pressure drop (wall shear stresses).

The steady flow curve obtained experimentally for the fluid C-25 was compared with the rheometric data. It was observed that the fluid presented values lower than the data measured in the rheometer, indicating a slip of the gel on the internal walls of the pipe. The data were corrected for the slip based on the truly shear volumetric flow rate (MACOSKO; LARSON, 1994; AKTAS et al., 2014), resulting in a better comparison with the rheometric data. Additionally, the behavior of fluid as shear stress is applied was analyzed by rheological creep tests. The results showed three states of deformation consistent with a solid-like behavior (region S) for low values of shear stress, i.e., lower than the yield stress. This behavior changed when the shear stress was slightly greater than the yield stress, and it was consistent with a region of coexistence of solid and fluid states (region S + F). Beyond yield stress, for greater shear stress values, the material showed a fluid behavior (region F). Finally, from the slip behavior observed in the evolution of the dimensionless velocity profiles, scaling was performed with other hydrodynamic quantities such as shear stress and velocity gradients in the wall. The data showed that the slip velocity is scaled in the form of a power-law only between the regions (S+F) and the region (F), due to that in the solid region (S), the slip velocity is independent of the values of shear stress and the velocity gradient. Based on the dependence of the slip velocity on the shear stress, a phenomenological picture of the slip behavior was established and the value of the thickness of the slip layer was estimated, whose value was on the order of microns, a minimal value for being observed within the resolution of the visualization technique used.

6. ACKNOWLEDGEMENTS

This work has been supported by the Federal University of Technology-Parana's Research Center for Rheology and Non-Newtonian Fluids-CERNN and Multilab LabReo-CERNN/UTFPR.

7. REFERENCES

Alba, K. and Frigaard, I., 2016. "Dynamics of the removal of viscoplastic fluids from inclined pipes". *Journal of Non-Newtonian Fluid Mechanics*, Vol. 229, pp. 43–58.

Benmouffok-Benbelkacem, G., Caton, F., Baravian, C. and Skali-Lami, S., 2010. "Non-linear viscoelasticity and temporal behavior of typical yield stress fluids: Carbopol, xanthan and ketchup". *Rheologica acta*, Vol. 49, No. 3, pp. 305–314.

Bingham, E.C., 1922. *Fluidity and plasticity*, Vol. 2. McGraw-Hill.

Bravo, R.R.S., De Negri, V.J. and Oliveira, A.A.M., 2018. "Design and analysis of a parallel hydraulic - pneumatic regenerative braking system for heavy-duty hybrid vehicles". *Applied Energy*, Vol. 225, No. 1, pp. 60–77.

Burfoot, D., Middleton, K. and Holah, J., 2009. "Removal of biofilms and stubborn soil by pressure washing". *Trends in Food Science & Technology*, Vol. 20, pp. S45–S47.

Buscall, R., 2010. "Letter to the editor: Wall slip in dispersion rheometry". *Journal of Rheology*, Vol. 54, No. 6, pp. 1177–1183.

Campos, R., 2018. *Design of quick couplings for drones and moving vehicles (in Portuguese)*. Master's thesis, Graduate Program in Mechanical Engineering, Federal University of Santa Catarina, Florianópolis, Brasil.

Carvalho, J.C.M., Martins, D., Simoni, R. and Simas, H., 2017. *Multibody Mechatronic Systems - Proceedings of the MUSME Conference held in Florianópolis, Brazil, October 24-28, 2017*. Mechanisms and Machine Science. Springer International Publishing.

Cole, P.A., Asteriadou, K., Robbins, P.T., Owen, E.G., Montague, G.A. and Fryer, P.J., 2010. "Comparison of cleaning of toothpaste from surfaces and pilot scale pipework". *Food and bioproducts processing*, Vol. 88, No. 4, pp. 392–400.

Coussot, P., 2014. "Yield stress fluid flows: A review of experimental data". *Journal of Non-Newtonian Fluid Mechanics*, Vol. 211, pp. 31–49.

Coussot, P. and Meunier, M., 1996. "Recognition, classification and mechanical description of debris flows". *Earth-Science Reviews*, Vol. 40, No. 3-4, pp. 209–227.

Curran, S., Hayes, R., Afacan, A., Williams, M. and Tanguy, P., 2002. "Properties of carbopol solutions as models for yield-stress fluids". *Journal of Food Science*, Vol. 67, No. 1, pp. 176–180.

Dalla, L.F., Soares, E.J. and Siqueira, R.N., 2019. "Start-up of waxy crude oils in pipelines". *Journal of Non-Newtonian Fluid Mechanics*, Vol. 263, pp. 61–68.

Damianou, Y., Philippou, M., Kaoullas, G. and Georgiou, G.C., 2014. "Cessation of viscoplastic poiseuille flow with wall slip". *Journal of Non-Newtonian Fluid Mechanics*, Vol. 203, pp. 24–37.

El-Gendy, H., Alcoutlabi, M., Jemmett, M., Deo, M., Magda, J., Venkatesan, R. and Montesi, A., 2012. "The propagation of pressure in a gelled waxy oil pipeline as studied by particle imaging velocimetry". *AIChE journal*, Vol. 58, No. 1, pp. 302–311.

EPE, 2020. "Brazilian energy balance 2020, final report (in portuguese)". Empresa de Pesquisa Energética EPE, Rio de Janeiro, epe.gov.br/sites-pt/publicacoes-dados-abertos/publicacoes/PublicacoesArquivos/publicacao-479/topico-528/BEN2020_sp.pdf. Accessed 12 January 2021.

Fernandes, R.B., Teixeira, J.S.V., Boeing, F., Pedro Filho, A., Berramashi, E.A., Tounier, M.B., Silva, M.B. and Caminha Junior, L., 2018. "System for monitoring controlled areas in work environments (in portuguese)". Patent, INPI - Instituto Nacional da Propriedade Industrial, Brazil, Utility Model, Registry number: BR10201806780403, Deposit: September 04, 2018.

Fryer, P., Christian, G. and Liu, W., 2006. "How hygiene happens: physics and chemistry of cleaning". *International Journal of Dairy Technology*, Vol. 59, No. 2, pp. 76–84.

Grando, M.T., 2017. *Complacency of cable guided robotic systems (in Portuguese)*. Ph.D. thesis, Graduate Program in Mechanical Engineering, Federal University of Santa Catarina, Florianópolis, Brasil.

Huilgol, R.R., Alexandrou, A.N. and Georgiou, G.C., 2019. "Start-up plane poiseuille flow of a bingham fluid". *Journal of Non-Newtonian Fluid Mechanics*, Vol. 265, pp. 133–139.

Kalyon, D.M., 2005. "Apparent slip and viscoplasticity of concentrated suspensions". *Journal of Rheology*, Vol. 49, No. 3, pp. 621–640.

Liu, Y. and de Bruyn, J.R., 2018. "Start-up flow of a yield-stress fluid in a vertical pipe". *Journal of Non-Newtonian Fluid Mechanics*, Vol. 257, pp. 50–58.

Macosko, C.W., 1994. "Rheology principles". *Measurements and Applications*.

Mendonça, P.T.R. and Fancello, E.A., 2019. *The method of finite elements applied to mechanics of solids (in Portuguese)*. Editora Orsa Maggiore, Florianópolis.

MLA, 2020. "MLA works cited: Electronic sources (web publications)". Modern Language Association, Purdue Online Writing Laboratory, Purdue University, owl.purdue.edu/owl/research_and_citation/mla_style/mla_formatting_and_style_guide/mla_works_cited_electronic_sources.html. Accessed 12 january 2021.

Møller, P., Fall, A. and Bonn, D., 2009. "Origin of apparent viscosity in yield stress fluids below yielding". *EPL (Europhysics Letters)*, Vol. 87, No. 3, p. 38004.

Pérez-González, J., López-Durán, J.J., Marín-Santibáñez, B.M. and Rodríguez-González, F., 2012. "Rheo-piv of a yield-stress fluid in a capillary with slip at the wall". *Rheologica acta*, Vol. 51, No. 11-12, pp. 937–946.

Phillips, D.A., Forsdyke, I.N., McCracken, I.R. and Ravenscroft, P.D., 2011. "Novel approaches to waxy crude restart: Part 2: An investigation of flow events following shut down". *Journal of Petroleum Science and Engineering*, Vol. 77, No. 3-4, pp. 286–304.

Piau, J., 2007. "Carbopol gels: Elastoviscoplastic and slippery glasses made of individual swollen sponges: Meso-and macroscopic properties, constitutive equations and scaling laws". *Journal of non-newtonian fluid mechanics*, Vol. 144, No. 1, pp. 1–29.

Poumaere, A., Moyers-González, M., Castelain, C. and Burghelea, T., 2014. "Unsteady laminar flows of a carbopol® gel in the presence of wall slip". *Journal of Non-Newtonian Fluid Mechanics*, Vol. 205, pp. 28–40.

Putz, A.M. and Burghelea, T.I., 2009. "The solid–fluid transition in a yield stress shear thinning physical gel". *Rheologica Acta*, Vol. 48, No. 6, pp. 673–689.

Roberts, G.P. and Barnes, H.A., 2001. "New measurements of the flow-curves for carbopol dispersions without slip artefacts". *Rheologica Acta*, Vol. 40, No. 5, pp. 499–503.

Santos, D.D., Furtado, G.M., Frey, S.L., Naccache, M.F. and de Souza Mendes, P.R., 2013a. "Flow of elasto-viscoplastic fluids inside a cavity". In *Proceedings of the 22nd International Congress of Mechanical Engineering - COBEM 2013*. Ribeirão Preto, Brazil.

Santos, D.D., Furtado, G.M., Frey, S.L., Naccache, M.F. and de Souza Mendes, P.R., 2013b. "Numerical investigation of elastic and viscous effects on inertial viscoplastic fluid flows". In *Proceedings of the 22nd International Congress of Mechanical Engineering - COBEM 2013*. Ribeirão Preto, Brazil.

Sierra, A.G., Varges, P.R. and Ribeiro, S.S., 2016. "Startup flow of elasto-viscoplastic thixotropic materials in pipes". *Journal of Petroleum Science and Engineering*, Vol. 147, pp. 427–434.

Simas, H. and Di Gregorio, R., 2019. "A technique based on adaptive extended jacobians for improving the robustness of the inverse numerical kinematics of redundant robots". *Journal of Mechanisms and Robotics*, Vol. 11, p. 020913.

Taghavi, S., Alba, K., Moyers-Gonzalez, M. and Frigaard, I., 2012. "Incomplete fluid–fluid displacement of yield stress fluids in near-horizontal pipes: experiments and theory". *Journal of Non-Newtonian Fluid Mechanics*, Vol. 167, pp. 59–74.

Younes, E., Bertola, V., Castelain, C. and Burghelea, T., 2020. "Slippery flows of a carbopol gel in a microchannel". *Physical Review Fluids*, Vol. 5, No. 8, p. 083303.

8. RESPONSIBILITY NOTICE

The following text, properly adapted to the number of authors, must be included in the last section of the paper: The author(s) is (are) solely responsible for the printed material included in this paper.